standard deviation of a measurement range from 0.02 to 0.41 percent over the 2–18-GHz frequency range. Also, it has been determined experimentally that one type of systematic error can be neglected.

Acknowledgment

The author extends his thanks and appreciation to Dr. G. F. Engen for technical guidance and assistance. Also, he acknowledges the significant contributions of T. Smith, III, who designed and developed the computer programs for the system control and measurement process; and C. Erskine and A. Lorenz who assisted with the instrumentation implementation.

References

[1] G. F. Engen and C. A Hoer, "Application of an arbitrary six-port junction to power measurement problems," *IEEE Trans. Instrum. Meas.*, vol. IM-21, pp. 470–474, Nov. 1972.

[2] C A. Hoer, "Using six-port and eight-port junctions to measure active and passive circuit parameters," U.S. Dept. Comm., Nat. Bur. Stand., NBS Tech. Note 673, Sept. 1975

[3] G. F. Engen, "Calibration of an arbitrary six-port junction for measurement of active and passive circuit parameters," *IEEE Trans. Instrum. Meas.*, vol. IM-22, pp. 295–299, Dec. 1973.

[4] N T. Larsen and F. R. Clague, "The NBS type II power measurement system," *Advances in Instrum*, vol. 25, pt 3, also Paper No. 712-70, in *Proceedings of the 25th Annual ISA Conference*, Philadelphia, PA, Oct. 26–29, 1970.

[5] E L Komarek and P V. Tryon, "An application of the power equation concept and automation techniques to precision bolometer unit calibration," *IEEE Trans. Microwave Theory Tech.*, vol. MTT-22, pt II, pp. 1260–1267, Dec. 1974.

Short Papers

A Cost-Effective Modular Downconverter for *S*-Band WEFAX Reception

H. PAUL SHUCH

Abstract—**The relocation of weather satellite facsimile downlinks from VHF into *S*-band has generated a requirement for reliable, low-cost microwave receiving equipment. This paper explores many of the design tradeoffs encountered in developing one such receiver system.**

Introduction to WEFAX

For the past decade, meteorological agencies around the world have received periodic weather facsimile (WEFAX) and automatic picture transmission (APT) printouts from a network of polar orbiting and geosynchronous satellites [1], [2]. The products available from these satellites are diverse, but generally include computer-gridded cloud cover maps such as the one shown in Fig. 1, derived from satellite-borne optical and infrared sensors [3]. Ground reception of such signals supports not only weather prediction, but also geological resource assessment and agricultural planning activities.

WEFAX coverage is currently limited to the western hemisphere, while APT is a worldwide, direct broadcast service. Users depending upon these transmissions include underdeveloped nations operating their ground receiving stations on an extremely limited budget and under the most adverse environmental conditions. The challenge facing the designer of WEFAX and APT receiving equipment thus involves assuring the utmost in reliability, ease of operation by unskilled personnel, and of course absolute minimum cost.

Manuscript received May 9, 1977; revised August 1, 1977

The author is with San Jose City College, San Jose, CA 95128, and MICROCOMM, 14908 Sandy Lane, San Jose, CA 95124.

Frequency Allocations

Several generations of weather satellites have transmitted frequency-modulated downlink signals in the 135–138 MHz region. A degree of standardization has begun to emerge with regard to image formatting, enabling users to recover multiple satellite products on a single receiver and display device, with minimum equipment modification. Perhaps a thousand commercial VHF weather satellite receiving stations now exist worldwide. Countless other, less elaborate systems have been fabricated by individual hobbyists and experimenters [4].

Spectrum allocation requirements, as well as a desire to escape ionospheric propagation anomalies, have dictated the assignment of downlink frequencies in the microwave region for the latest series of meteorological satellites. The first two of these Designated Synchronous Meteorological Satellite/Geostationary Operational Environmental Satellite (SMS/GOES), have been deployed by the U.S. National Oceanic and Atmospheric Administration (NOAA). They have recently been joined in geostationary orbit by GMS, the Japanese weather satellite, and will be supplemented shortly by two additional geostationary satellites now being developed by the USSR and the European Space Agency (ESA). The five spacecraft will be positioned above the equator approximately seventy degrees apart, thus providing nearly global WEFAX coverage.

All of these satellites will transmit WEFAX at a frequency near 1.7 GHz, with modulation characteristics and image format being fully compatible with present VHF WEFAX transmissions. In order to assure maximum utilization of existing equipment, linear downconversion has emerged as an accepted technique for developing worldwide *S*-band WEFAX receiving capability.

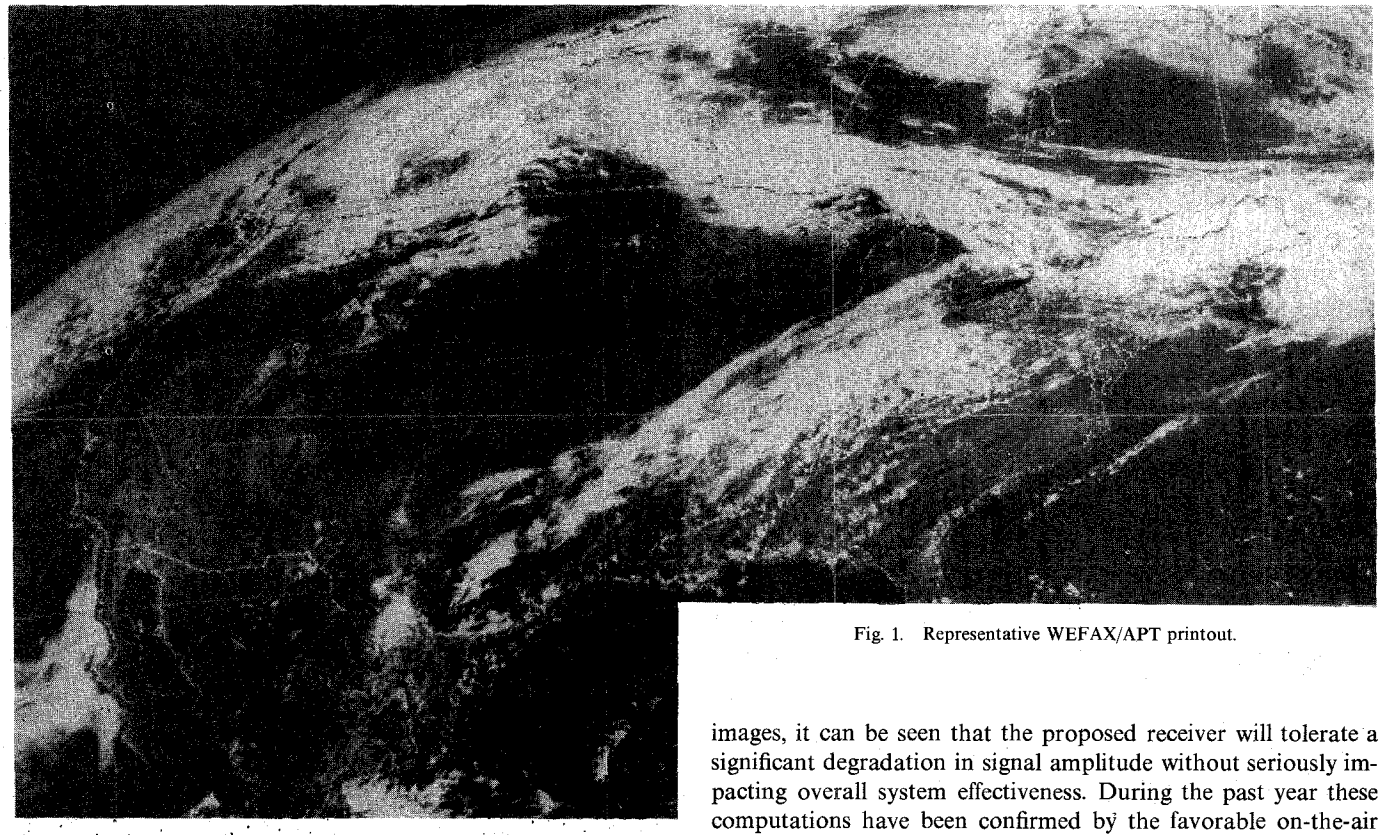

Fig. 1. Representative WEFAX/APT printout.

TABLE I
SYSTEM SIGNAL-TO-NOISE CALCULATIONS

1.	Given: EIRP (Satellite) = +54.4 dBm
2.	Path Loss (dB) = 92.5 + 20 $\log_{10}$ d + 20 $\log_{10}$ f where f = 1.7 (GHz) and d = 35,788 (Km) Thus Path Loss = -188.2 dB.
3.	Power to Receive Antenna = EIRP + Path Loss = -133.8 dBm.
4.	Given: a 1.2 m. dia. parabolic reflector, with 55% feed efficiency, Antenna Gain = +25 dBi.
5.	Recovered Power = Power to Antenna + Gain = -108.8 dBm.
6.	Assuming that T_o = 290 ^oK, Minimum Discernible Signal (MDS) = -174 dBm + 10 $\log_{10}$ BW + 10 $\log_{10}$ F where BW = 2.6 x 10^4 (Hz), and F = 2.2 Thus MDS = -126.4 dBm
7.	SNR = Recovered Power - MDS = 17.6 dB.

PATH CALCULATIONS AND SYSTEM MARGIN

System noise margins for a proposed *S*-band WEFAX receiver are derived in Table I. Significant assumptions are the satellite's Effective Isotropic Radiated Power (EIRP), the use of a small (1.2 m) parabolic reflector and feed as the groundstation antenna, an IF bandwidth of 26 kHz in the VHF receiver, and a receiver overall noise factor of 2.2 (which represents a noise figure of 3.4 dB), a design goal for the proposed downconverter. Under these conditions, the system's signal-to-noise ratio (SNR) approaches 17 dB.

Since a 10–12-dB SNR will yield relatively noise-free WEFAX images, it can be seen that the proposed receiver will tolerate a significant degradation in signal amplitude without seriously impacting overall system effectiveness. During the past year these computations have been confirmed by the favorable on-the-air performance of a number of user's systems.

SYSTEM MODULARIZATION

During initial development of the WEFAX downconverter, numerous mixers, bandpass filters, single stage amplifiers, local oscillators and multipliers were fabricated, each in a separate shielded enclosure, all with input and output ports connectorized and matched to a 50 Ω, nonreactive interface impedance. Circuitry for each of these modules was based upon various of the author's previously published designs, adapted to the frequency of interest [5]–[8]. It should be pointed out that an analytical design approach based upon scattering-parameter analysis was employed; more simplistic design techniques based upon frequency scaling are frequently fraught with difficulty.

Performance of individual modules was generally optimized empirically prior to their inclusion in a system prototype. This modular approach allowed maximum flexibility in configuring the system for optimum performance consistent with minimizing costs. Wherever possible, it was decided to cascade identical modules rather than develop a wide variety of circuits. The resulting system, shown in Fig. 2, satisfied the major sensitivity, selectivity, stability, and spectral purity criteria, proved readily repeatable, and required little or no realignment of the individual circuits following system integration.

The modular concept was carried forward into production, thus minimizing manufacturing costs, maximizing isolation between stages, and enhancing both user flexibility and maintainability. For example, each downconverter contains three identical amplifiers, as well as three identical bandpass filter modules. Thus the required inventory of field-replaceable assemblies is minimized, and troubleshooting by stage substitution becomes a viable means of reducing system downtime.

Fig. 3 depicts an assembled downconverter, patterned after the block diagram of Fig. 2. Also shown are views of the individual modules employed.

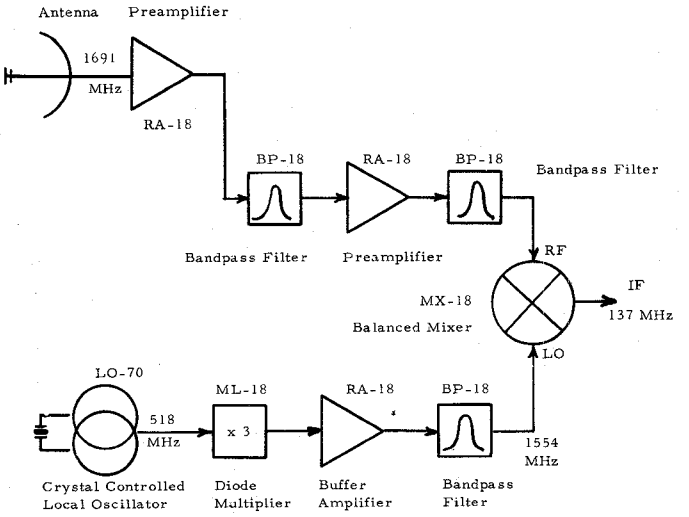

Fig. 2. System block diagram of the MICROCOMM modular *S*-band WEFAX downconverter.

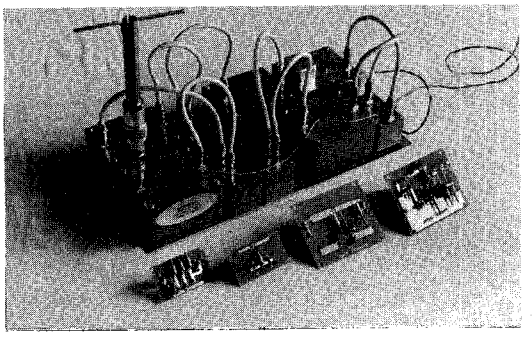

Fig. 3. Completed downconverter assembly, with individual modules in foreground.

Cost Considerations

NOAA, in a recent technical memorandum, described a workable downconverter for *S*-band WEFAX reception, based upon readily available standard microwave assemblies [9]. It appeared clearly possible to reduce the cost of this converter by at least a factor of three, while significantly improving system performance, by developing the most cost-effective circuits tailored to the particular application.

Link analysis (see Table I) confirmed the feasibility of recovering noise-free images with a much smaller antenna than the one used by NOAA, by somewhat upgrading receiver performance requirements. Two stages of bipolar amplification preceding a passive balanced mixer proved practical to achieve the required receiver sensitivity. Conjugately matched amplifiers were used, thus simplifying their design and assuring improved stability. Of course, it was first necessary to confirm by noise circle analysis that such impedance-matched preamplifiers would not degrade system noise figure beyond the 3.4-dB design goal [10].

Bandpass filtering at the various mixer ports made it possible to use a singly balanced mixer configuration, while maintaining the same system-spurious rejection as the NOAA system had exhibited with its more costly double-balanced mixer. Filtering in the preamplifier chain also eliminated image noise, while significantly enhancing dynamic range.

Although frequency-stability requirements demanded the use of a crystal-controlled local oscillator chain, it was found that employing Automatic Frequency Control (AFC) in the VHF receiver could compensate for minor LO drift. Thus the temperature stability requirements of the local oscillator were relaxed somewhat, resulting in further cost savings.

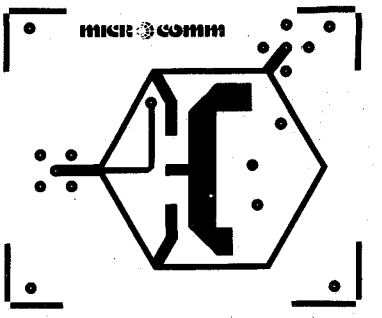

Fig. 4. Typical microstripline artwork.

By applying a predetermined dc bias to the LO multiplier diode, its conduction angle was optimized to enhance third-harmonic output (while reducing other spectral components). This technique reduced the filtering requirements of the local oscillator chain.

To minimize module fabrication costs, microstripline construction was employed throughout. However, rather than etch these circuits on the traditional (and costly) controlled ε_r microwave substrates, low-cost fiberglass-epoxy printed circuit stock was used. Dissipative losses were clearly measurable, but tolerable, while anomalies due to substrate discontinuities were readily compensated by tuning adjustments. Several hundred of these modules have been successfully fabricated, using photo-etching techniques along with artwork such as that shown in Fig. 4.

The following paragraphs describe some of the design details and performance characteristics of the individual WEFAX modules.

Preamplifiers

Each amplifier module consists of a single common-emitter stage. The transistor utilized is an ion-implanted bipolar device from Hewlett-Packard, packaged in a rugged 100-mil-square stripline package. The quiescent bias point ($V_{ce} = 10$ V, $I_c = 15$ mA) is established by an on-card Zener stabilization circuit, and was selected in an attempt to trade off the mutually exclusive requirements of optimum noise figure and input match.

At the bias point used Γ_0, the source reflection coefficient for optimum noise figure, is found to be quite close on the Smith chart to the value found for Γ_s, source reflection coefficient for simultaneous conjugate match. Thus degradation from optimum stage noise figure, when the input is matched to 50 Ω, is on the order of 0.5 dB.

Input and output matching circuits are of the familiar shunt-stub variety, with 50-Ω open microstriplines of the required length positioned along 50-Ω input and output lines, at a predetermined position with respect to the transistor package. The resulting networks transform the transistor's die characteristics and package parasitics to 50 Ω at the operating frequency, with input and output VSWR of less than 2 to 1.

The amplifier design, including dimensioning of the required microstriplines, was performed on a Hewlett-Packard Model 25 programmable calculator, utilizing programs developed by the author for this purpose.[1]

[1] Further information on these programs is available from the author for the courtesy of a stamped self-addressed envelope.

The relatively high quiescent collector current used in this amplifier design results in a wide dynamic range, providing +10 dBm output at the 1-dB compression point. This large-signal capability enabled the amplifier to be used to raise the local oscillator chain injection level, as indicated in Fig. 2.

The assembled amplifier module measures 2 × 2½ × 3 in, draws 16 mA from a +12 V dc supply, and offers 12-dB gain and a 2.8-dB noise figure at 1.7 GHz.

Balanced Mixer

The mixer circuit employed in this downconverter utilizes a pair of Schottky-barrier diodes in a single-balanced configuration, with RF and LO signals coupled to the diodes by a $3/2\lambda$ 180° ring hybrid, of "rat race." The hybrid coupler is implemented in microstripline, hexagonally rather than in the traditional circular configuration (see Fig. 4). In selecting this hybrid over the single or double section quadrature "branch coupler," extended ring hybrid, or other possible approaches, attention was paid to impedance match, phase and amplitude imbalance, coupler losses, and isolation characteristics of each type, over at least a 20 percent bandwidth. It is believed that the $3/2\lambda$ ring represents a workable compromise from the standpoint of both performance and ease of manufacture.

For optimum conversion efficiency, this mixer requires 3 to 5 mW of local oscillator injection. The mixer then exhibits 7-dB single sideband (SSB) conversion loss, and greater than 25-dB LO-to-RF isolation. The packaged mixer measures 2 × 2½ × 3 in.

Bandpass Filter

Multipole interdigital bandpass filters of edge-coupled stripline construction have received considerable attention in recent years. However, this project demanded a low-cost noncritical, tunable filter to be cascaded between the various modules. What ultimately emerged is a microstripline variant of the once-popular half-wave coaxial resonator. A shortened half-wave microstripline is grounded at both ends, capacitively center-loaded, and tapped at the 50-Ω points for input and output connection. This results in a single-pole filter of modest Q and gradual skirts, but extremely low insertion loss. When cascaded after each of the two preamplifiers, as shown in Fig. 2, image rejection exceeds 25 dB. And when used at the mixer's LO port, this simple filter attenuates the closest spurious components by at least 40 dB.

The packaged filter measures 1 × 1⅜ × 2¼ in, is tunable from 1.5 to 2.3 GHz, and exhibits typically 0.5-dB insertion loss with a loaded Q of 20.

Local Oscillator

The primary requirements for any microwave local oscillator are stability and spectral purity. An equally important consideration, frequently overlooked, is calibration tolerance. That is, if a given satellite link is to be downconverted into a fixed IF, for detection by a nontunable receiver, it is important to assure that the downconverted signal appears centered in the passband of the IF. Since any attempt to VXO or "rubber" the crystal's frequency of oscillation is to be avoided in the interest of stability, this demands precision in the frequency calibration of the crystal, *in the particular oscillator circuit used.*

Crystal manufacturers can generally optimize custom-ground crystals for operation in any circuit, provided a schematic and/or test fixture is supplied. An alternative cost-effective technique employed in this design is to use an oscillator circuit of the crystal manufacturer's choosing. In so doing, it is found that crystals of widely separated production runs all fall well within the specified calibration tolerance of ±0.001 percent, as well as the required thermal stability spec of ±0.002 percent from −10 to +60°C.

It should be noted that the above specifications imply an LO frequency variation of ±15 kHz at room temperature, and ±30 kHz over environmental extremes. Since the IF bandpass specified for VHF WEFAX receivers is typically 26 kHz, it is obvious that some type of Automatic Frequency Control (AFC) circuitry within the IF receiver is required to provide capability to lock onto and track incoming S-band WEFAX transmissions over the operating temperature range.

If AFC is not used, some degree of thermal stabilization for the local oscillator module should be provided by the user. In terms of overall cost, it appears more practical to AFC the VHF receiver than to add the oven, proportional controller, and ancillary circuitry needed for temperature stabilization.

The circuitry selected for the LO module consists of a common-base modified Colpitts oscillator utilizing a series-resonant overtone crystal at a frequency near 130 MHz. Output power is kept low (on the order of 0.5 mW) to avoid undue crystal heating. This signal is doubled to 259 MHz in a class-C common emitter stage operated at 6-dB gain, filtered, doubled again to 518 MHz in a similar stage, and applied to a two-pole microstripline bandpass filter. The 518 MHz output has spurious rejection exceeding 40 dB, at an output power of 5–10 mW. This signal is applied to a diode tripler incorporating two poles of bandpass filtering and positive diode bias, as discussed previously; thence to a buffer amplifier and additional filtering at 1554 MHz, as shown in Fig. 2.

System Integration

In order to establish a low overall system noise figure, the first preamplifier of the S-band downconverter is generally mounted directly at the antenna feed. A moderate length of high-quality coaxial cable can then be run from the first preamplifier to the balance of the downconverter, which may be located indoors. Thus the bulk of the modules need not be environmentally protected, further reducing their cost. However, it is necessary to weather-proof the first antenna-mounted preamplifier. Many commercial antenna assemblies include a small weatherproof enclosure for just this purpose, either at the focus of the parabolic reflector or mounted on its back. Where no such enclosure is provided, it is found that plastic kitchenware boxes, such as the Tupperware sandwich box, are entirely satisfactory for protecting the antenna-mounted preamplifier.

Tradeoffs such as the Tupperware box, and various of the circuit design and fabrication techniques outlined here, may appear crude to the engineering purist. Nonetheless, they represent a reasonable attempt to achieve state-of-the-art receiver performance on a highly restricted budget—the *primary* design objective for the S-band WEFAX downconverter.

Summary

A method has been described for downconverting S-band WEFAX, for reception by an existing VHF weather satellite groundstation. Prudent design tradeoffs have held total costs, including the required antenna and feed, RF modules, and interconnecting cables, to around $1000.

References

[1] J. J Fortuna and L N Hambrick, "The operation of the NOAA polar satellite system," NOAA Tech Memo. NESS 60, Nov 1974

[2] W. J. Hussey, "The geostationary environmental satellite system," in *EASCON '74 Conf. Rec*, pp. 490–496

[3] E. R Hoppe and A. L. Ruiz, "Catalog of operational satellite products," NOAA Tech Memo NESS 53, Mar 1974

[4] Dr. R. E. Taggart, *Weather Satellite Handbook*. Peterborough, NH: 73 Inc, 1976.

[5] H. P. Shuch, "1296 MHz transceiver," *Ham Radio*, pp. 8–23, Sept. 1974.
[6] ——, "UHF double balanced mixers," *Ham Radio*, pp. 8–15, July 1975.
[7] ——, "High performance conversion module for the 23-cm band," *Radio Handbook*, 20th ed. Indianapolis, IN: Howard Sams & Co., 1975, pp. 20–66.
[8] ——, "Solid state microwave amplifier design," *Ham Radio*, pp 40–47, Oct 1976
[9] J. J. Nagle, "A method of converting the SMS/GOES WEFAX frequency (1691 MHz) to the existing APT/WEFAX frequency (137 MHz)," NOAA Tech. Memo NESS 54, Apr. 1974.
[10] "Noise parameters and noise circles for the HXTR-6101, -6102, -6103, -6104, and -6105 low noise transistors," Application Bulletin 17, Hewlett-Packard Company, Jan 1977.

Theoretical Analysis of a Ridged-Waveguide Mounting Structure

SHIZUO MIZUSHINA, MEMBER, IEEE,
NOBUO KUWABARA, MEMBER, IEEE,
AND HIROSHI KONDOH, MEMBER, IEEE

Abstract—**The driving-point impedance of a single-gap thin conductor strip, a model of the ribbon-and-pedestal of diode package, mounted across the gap of a ridged waveguide has been derived using the induced EMF method. The dyadic Green's function for the ridged waveguide is derived to facilitate the analysis. An equivalent circuit is developed which involves an infinite array of transformers representing the couplings between the conductor strip and the waveguide normal modes. Numerical results for a typical example are presented to discuss the validity of the analytical results and also to demonstrate a remarkably smooth behavior of the driving-point impedance of the mount over a frequency range from 5.4 to 25.4 GHz.**

Introduction

Ridged waveguides have been used for many years in microwave components and systems requiring broad bandwidths. Among such applications, mounting structures for solid-state devices are of our interest here [1], including the fin-line components [2]. A recent experimental investigation showed that mechanical tuning ranges of 8.5–26 GHz and 14–28 GHz were achieved with packaged Gunn and IMPATT diodes, respectively, mounted in the ridged-waveguide cavities [3], [4]. This gave us a motivation to study the ridged-waveguide mounting structure theoretically as well. An attempt was made to extend the induced EMF method, which had been successfully applied to the rectangular waveguide post-coupling structure [5], [6], to a ridged-waveguide mounting structure where a packaged diode fitted into the gap spacing between the ridges extending uniformly in the z direction. In this short paper we analyze a simplified model of the mount, in which the package ceramic ring is disregarded and the ribbon-and-pedestal of the diode is represented by an equivalent flat conductor strip, as in [5], [6], to derive its driving-point impedance.

Analysis

A cross section of the ridged-waveguide mounting structure is sketched in Fig. 1(a) and the model used in the analysis in Fig. 1(b) along with the coordinate system. The conductor strip with a width w, a gap g, and an infinitesimal thickness at $z = 0$ is regarded as a small antenna radiating into the ridged waveguide. The electric field in the guide $\boldsymbol{E}(\boldsymbol{R})$ generated by the current density $\boldsymbol{J}(\boldsymbol{R})$ in the conductor strip can be derived by

$$\boldsymbol{E}(\boldsymbol{R}) = -j\omega\mu_0 \int_{\text{vol}} \bar{\boldsymbol{G}}(\boldsymbol{R}/\boldsymbol{R}') \cdot \boldsymbol{J}(\boldsymbol{R}/\boldsymbol{R}')\, dv' \tag{1}$$

provided that the Green's function, $\bar{\boldsymbol{G}}(\boldsymbol{R}/\boldsymbol{R}')$, is known. It is possible to derive $\bar{\boldsymbol{G}}(\boldsymbol{R}/\boldsymbol{R}')$ for the ridged waveguide using the Ohm–Rayleigh method described by Tai in [7] with the aid of the knowledge of the complete eigenfunctions of the ridged waveguide given by Montgomery in [8]. Quoting from [8], we can write for the y component of the electric basis field in region 1, referring to Fig. 1(b), as

$$e_{Hy}(\boldsymbol{R}) = -\sum_{n=0}^{\infty} \eta_{1n} k_{x1n} \cos k_{x1n} x \cos \frac{n\pi}{b_3}(y - b_3) \tag{2}$$

for TE modes and

$$e_{Ey}(\boldsymbol{R}) = \sum_{n=1}^{\infty} \xi_{1n} \frac{n\pi}{b_3} \cos k_{x1n} x \cos \frac{n\pi}{b_3}(y - b_3) \tag{3}$$

for TM modes where k_{x1n} is defined by

$$k_{x1n} = \begin{cases} \sqrt{k_T^2 - \left(\dfrac{n\pi}{b_3}\right)^2}, & k_T \geq \dfrac{n\pi}{b_3} \\ -j\sqrt{\left(\dfrac{n\pi}{b_3}\right)^2 - k_T^2}, & k_T < \dfrac{n\pi}{b_3} \end{cases} \tag{4}$$

with

$$\Gamma = \begin{cases} \sqrt{k^2 - k_T^2}, & k \geq k_T \\ -j\sqrt{k_T^2 - k^2}, & k < k_T \end{cases} \tag{5}$$

and $k = \omega\sqrt{\varepsilon_0 \mu_0}$.

In the above expressions, we adopted the convention $\exp(j\omega t - j\Gamma z)$ for the wave propagating in the positive z direction and the subscripts H and E for the TE and the TM modes, respectively. In (2) and (3) we retained only those modes which satisfy the magnetic-wall-boundary condition at the symmetry plane of the waveguide since the current is centered at this plane. In (4), k_T is an eigenvalue and k_{x1n} is the propagation constant in the x direction of the spatial harmonic component in region 1 associated with the eigenvalue. The amplitudes of these spatial

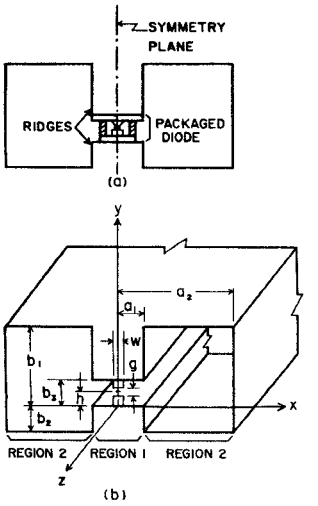

Fig. 1. A ridged-waveguide mounting structure. (a) A cross-sectional sketch of the mount. (b) The model used in the analysis

Manuscript received May 13, 1977, revised July 22, 1977

S. Mizushina and H. Kondoh are with The Research Institute of Electronics, Shizuoka University, Hamamatsu 432, Japan

N. Kuwabara was with The Research Institute of Electronics, Shizuoka University, Hamamatsu 432, Japan. He is now with the Electrical Communication Laboratories, Nippon Telegraph and Telephone Public Corporation, Tokai-mura, Ibaragi-ken 319-11, Japan.